Value of C-arm computed tomography in radiofrequency ablation of small lung lesions

X.Q. Li, Y. Zhang, D.B. Huang, J. Zhang, G.S. Zhang, Z.X. Wen, J.H. Li and H.L. Liu

Department of Interventional Radiology, Zhongshan City Peoples' Hospital, Zhongshan, Guangdong Province, China

Corresponding author: X.Q. Li
E-mail: xiaoqunlicn@163.com

ABSTRACT. This study aimed to explore the value of C-arm computed tomography (CT) applications in radiofrequency ablation (RFA) of small lung lesions. The puncture success rate, cumulative survival rate, tumor response rate, complications, and radiation dose during C-arm CT-guided RFA of 36 small lung lesions in 34 patients were analyzed. In 35 RFA procedures for 36 small lung lesions, the puncture success rate was 100%. There were 7 cases of complications, including 4 cases of pneumothorax (puncture suction or closed chest drainage was not required) and 3 cases of hemoptysis. The cumulative survival rate in the 34 patients after RFA was 100% at 6 months, 69.0% at 1 year, and 60.0% at 2 years. In assessments of 36 foci imaged during the follow-up period, the total response rates at 1 month, 3 months, and 6 months were 77.8% (28/36), 69.7% (23/33), and 61.3% (19/31), respectively. The mean cumulative dose and average effective dose during surgery were 120.1 ± 61.4 mGy and 3.5 ± 1.7 mSv, respectively. The application of C-arm CT to RFA of small lung lesions could provide abundant information to the surgeon

and increase the lesion puncture success rate and is considered to be a promising image-guided technology.

Key words: C-arm CT; Small lung lesions; Radiofrequency; Radiation dose

INTRODUCTION

According to data issued by the World Health Organization (WHO) in September, 2011, the incidence and mortality of lung cancer is the highest among all kinds of malignant tumors, and the number of deaths from lung cancer has exceeded the total number of deaths from breast cancer, prostate cancer, and colorectal cancer combined. Therefore, lung cancer has become a serious public health problem (Ferlay et al., 2010). Traditional methods for treatment of lung cancer mainly include surgery, chemotherapy, radiotherapy, and so on; however, a significant number of patients are non-surgical candidates resulting from co-morbidities or limited pulmonary reserve (Sharma et al., 2011). Recent years have witnessed the development of radiofrequency ablation (RFA) as a minimally invasive technology for tumor ablation, which plays a more and more important role in topical treatments for lung tumors (Simon et al., 2007). To some extent, it has been considered as an alternative to surgery for patients with lung cancer who are not eligible for surgery, and for those who have lost or refused surgery opportunities.

In clinical practice, there is difficulty in accurately locating small lung lesions with RFA. At present, commonly used image-guided technologies consist of digital subtraction angiography (DSA), computed tomography (CT), and B-mode ultrasonography. However, limitations of these technologies in the accurate localization of small lung lesions have been identified. It is easy to perform DSA, but difficult to precisely locate small lung lesions, especially lesions in deep positions. The advantages of CT guidance include relatively high time and space resolutions as well as accurate puncture guidance, but it only provides static cross-sectional images instead of real-time monitoring. B-mode ultrasonography-guided puncture achieves real-time monitoring without radiation exposure, but is only suitable for lesions located in the lung periphery adjacent to the chest wall or in the mediastinum.

In recent years, newly developed C-arm CT technology has exhibited obvious advantages over the abovementioned image-guided approaches. The movement of the puncture needle can be observed by C-arm CT in a real-time, dynamic method on high-resolution CT imaging, which allows the clinician to observe the size, shape, and structure of the lesions and their relationships with peripheral tissues in 3 dimensions. This technology also enables the surgeon to avoid barriers and dangerous positions, to observe and puncture lesions smaller than 3 cm, as well as to monitor for complications and evaluate therapeutic efficacy.

At present, there have been only a few published papers regarding C-arm CT applications in clinical practice. Therefore, it is of great clinical value to investigate how to simplify RFA procedures using C-arm CT, both to improve the accuracy of positioning electrode needles and to reduce radiation exposure to both patients and clinicians. We aimed to optimize the surgical procedure through extensive research and to provide scientific evidence for C-arm CT applications.

MATERIAL AND METHODS

Clinical data

C-arm CT-guided RFA was performed to ablate lung tumor lesions with maximum diameters of 3.0 mm in 34 patients, including 20 men and 14 women in the Radiology Department of People's Hospital of Zhongshan between November 2007 and June 2012. The ages of the patients ranged from 28 to 80 years old, with an average of 56 ± 3 years and a median age of 60 years. Among the 36 tumors, the maximum diameter was between 0.4 and 3.0 cm, with an average of 1.8 ± 0.7 cm; in 21 cases, the size was smaller than 2 cm. RFA was performed 35 times in 34 patients with a repetition in 1 patient. This study was conducted in accordance with the Declaration of Helsinki and was conducted after approval of the Ethics Committee of Zhongshan City Peoples' Hospital. Written informed consent was obtained from all participants.

Operation procedure

The general characteristics of the patients were assessed before the operation, including cardiopulmonary insufficiency, infection, and hemorrhage history, as well as the usage of anticoagulants, bronchodilators, etc. Surgical candidates were not allowed to eat before the operation, and 50 mg pethidine was injected intramuscularly at the beginning of the operation.

Recent imaging examinations, such as CT or magnetic resonance image, were used to assess tumor size, location, peripheral structure, and so on. The patient's body was placed in an appropriate position, such as a supine, prone, or lateral position according to the tumor location in the lungs, to shorten the vertical distance between the lesion and the corresponding point on the skin for needle insertion and to avoid anatomical structures including the costae, large vessels, lung bullae, interlobar fissures, large tracheas, and scapulae.

The patients raised themselves using both hands and the quasi-puncture area on the body surface was labeled with gridded metal markers fabricated in-house to facilitate the localization of lesions. The patients underwent respiratory training in an attempt to facilitate respiratory movement consistency as much as possible. Three-dimensional (3-D) rotation scanning was performed with a C-arm CT (GE INNOVA 3100 IQ, Fairfield, CA, USA; PHILIPS 1250-FD20, Amsterdam, Netherlands) with a speed of 20 or 40°/s over a total of 200°. The acquired image data were transmitted to an AW workstation (General Electric company) for 2-D and 3-D reconstruction. The reconstructed multiplanar imaging showed the tumor position, shape, and range. With measurement tools provided on the workstation, we drew the needle path to the target lesion on the body surface, measured the depth of the inserted needle, and selected a suitable puncture point on the body surface according to the lesion characteristics combined with the gridded metal markers (Figure 1A-D). The puncture point was labeled on the patient's body; the surgical site was then sterilized and draped with an operation towel. A concentration of 2% lidocaine was injected into the puncture point to achieve a local infiltration of anesthesia from the skin to the parietal pleura, and the syringe needle was left in the chest wall after the administration of local anesthesia. The relationship between the needle and lesion position was preliminarily assessed.
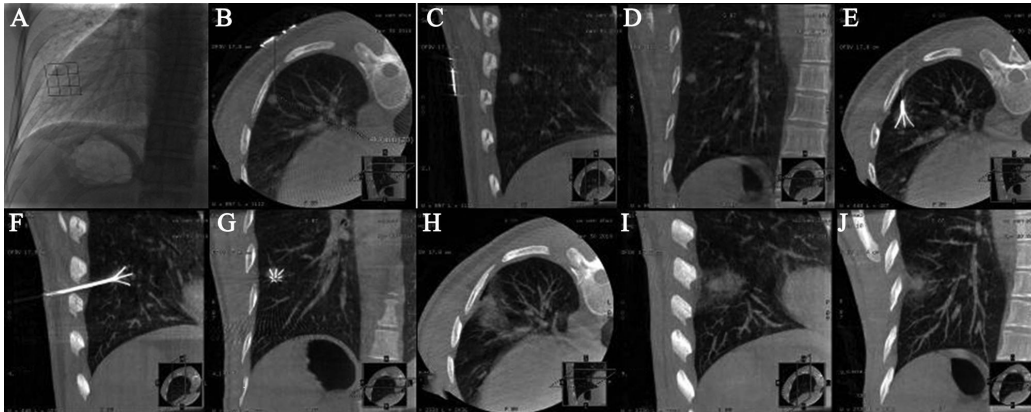
Figure 1. Radiofrequency ablation procedure to ablate small lung lesions. **A.** Preoperative location; **B.-D.** axial, sagittal, and coronal images acquired by 3-D reconstruction; the needle path drawn at the target point and the corresponding body surface point using workstation tools; the measured depth of the inserted needle; **E.-G.** relocation of the needle-electrode after expansion; **H.-J.** review of the ablated lesion immediately following the procedure.

The patients held their breath while the ablation needle (StarBurst XL needles, RITA Medical Systems, Mountain View, CA, USA) punctured through the muscular layer from the marked point to the measured depth, followed by fixation of the ablation needle. Three-dimention rotation scanning was performed, and a 3-D image was reconstructed to examine whether the needle tip was located in the tumor at a suitable position from multiple directions; if not, the needle was adjusted to a proper position followed by a repetition of scanning.

Once the tip of the ablation needle was located in the middle of the tumor, the anchor coupled to the electrode needle was opened, which can avoid inaccurate orientations caused by tumor movement resulting from opening the needle-electrode. To observe the needle-electrode opening, 3-D scanning and image reconstruction were performed once again; RFA was conducted when the needle-electrode was in a suitable position (Figure 1E-G).

The ablation apparatus (Model 1500X RF Generator, RITA Medical Systems) started with a radiofrequency generator power of 150 W and an initial ablation temperature of 90°C, which increased to 103°C during ablation. The ablation time was set to 15-25 min according to lesion size in the lungs. When the diameter of tumor is larger than 5 cm, the ablation should be performed several times from different points and surfaces to enhance the damage rate of the lesion. A total of 50 mg pethidine was injected intramuscularly if the patient felt strong pain during the surgery.

After the operation, 3-D scanning and 3-D image reconstruction were performed again to observe the lesion and evaluate the ablation as well as complications, such as hemorrhage and pneumothorax (Figure 1H-J).

Assessment of radiation dose

The DAP (dose area product) value (cGy·cm^2) was recorded for each operation and

each patient; the effective dose (ED; mSv) was calculated according to a Monte-Carlo simulation of a conversion coefficient (ICRP, 2007). The formula was:

$$ED = \text{conversion coefficient (k) x DAP, where k} = 0.14 \text{ mSv·Gy}^{-1}\text{·cm}^{-2}$$

Evaluation method for lung tumor RFA efficacy

Our research adopted a modified response evaluation criteria for solid tumors (Fernando et al., 2005), which consisted of complete response, partial response, stable disease, and progressive disease, as summarized in Table 1. CT reviews were performed at 1, 3, and 6 months after the operation.

Table 1. Modified response evaluation criteria for solid tumors (RECIST) used to evaluate treatment response.

Effect	CT tumor size (RECIST)	CT tumor density	PET
CR (any 2)	Lesions disappeared or scar <25% initial	Cystic change or cavity formation	SUV <2.5
PR (any 1)	Reduction of maximum diameter >30%	Decreased density in the lesion, central necrosis with liquid core	SUV decreased
SD (any 1)	Reduction of maximum diameter <30%	Solid tumor, no central necrosis or cavity formation	SUV did not change
PD (any 2)	Increase of maximum diameter >20%		

SUV = standard uptake value of ^{18}F fluorodeoxyglucose on a PET scan. CR = complete response; PR = partial response; SD = stable disease; PD = progressive disease.

Statistical analysis

The SPSS version 16.0 software (International Business Machines Corporation) was utilized to perform a statistical analysis of the cumulative survival rate, response rate, and complication rate, as well as the cumulative dose of surgical radiation and the effective dose.

RESULTS

Among a total of 35 RFA surgeries in our research, a puncture success rate of 100% was observed among the 36 lesions with 7 cases of complications, including 4 cases of pneumothorax (puncture suction or closed chest drainage was not required) and 3 cases of hemoptysis. The follow-up time ranged from 2 to 56 months with an average of 16.5 ± 13.1 months. Nine patients died during follow-up, and 25 patients survived until the end of the follow-up study (August 31, 2012), with a follow-up rate of 100% (34/34). According to the life table method, the accumulated survival rate at 6 months, 1 year, and 2 years was 100.0, 69.0, and 60.0%, respectively (Figure 2).

In the assessment of 36 foci imaged during the follow-up period, the total response rate at 1, 3, and 6 months was 77.8% (28/36), 69.7% (23/33), and 61.3% (19/31), respectively. The mean accumulated dose and mean effective dose in the operations were 120.1 ± 61.4 mGy and 3.5 ± 1.7 mSv, respectively.
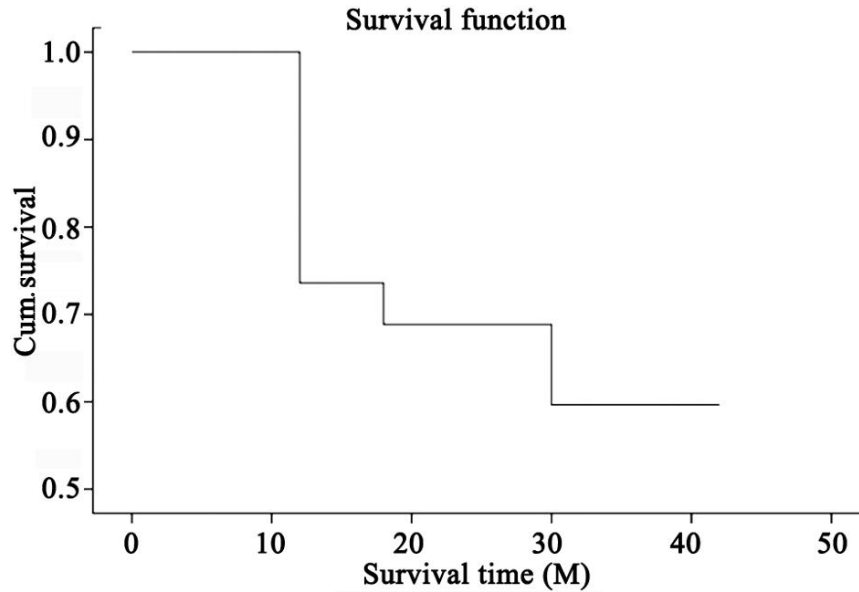
Figure 2. Cumulative survival rate of the 34 patients after radiofrequency ablation (life table method).

DISCUSSION

C-arm CT is an innovative imaging technology, known as 3-D C-arm CT or flat-panel tomographic angiography imaging technology, and demonstrates inconsistent names across different brands, such as syngo DynaCT (Siemens AG, Healthcare Sector, Forchheim, Germany), XperCT (Philips Healthcare, Andover, MA, USA), and Innova CT (GE Healthcare, Chalfont St. Giles, UK). In the meantime, a number of terms have emerged in the literature to describe this new imaging technology, including C-arm CT, cone beam CT, cone-beam volume CT, volume CT, angiographic CT, flat-panel CT, and others (Orth et al., 2008).

Among several common image-guided RFA modalities for small lung lesions, C-arm CT exhibits many advantages. It is relatively easy to perform percutaneous lung puncture under DSA guidance (Manhire et al., 2003), which acquires the optimal puncture path by adjusting the patient position or projection angle of the bulb tube, and additionally allows for observations of the depth and direction of needle puncture in the lung so as to achieve the ideal puncture effect. Moreover, the clinician has more space to perform RFA in a shorter time. However, this method has shown disadvantages in puncture accuracy, as well as in predicting the path and depth of puncture. Moreover, DSA has difficulty in identifying lesions smaller than 10 mm or lesions adjacent to blood vessels or the mediastinum (Hwang et al., 2010), as well as in recognizing minor complications in sufficient time.

CT-guided RFA possesses good repeatability, a wide field-of-view, relatively high time and space resolutions, and excellent accuracy. However, CT cannot be utilized for real-time monitoring and requires the clinician to determine the puncture direction based on their abundant personal experience. In addition, repeat scanning is necessary, yet can only provide a static cross-sectional image, which is unable to reflect the relation of the lesion to neighbor-

ing structures on the Z-axis, or to observe the lesion in 3-D. Although CT perspective can make up for this disadvantage, it requires a quite large dose of radiation. Sometimes the non-cooperation of patients and breath movement results in the disappearance of the target during the puncture procedure, especially in the basal parts of the lung. This situation presents more often with relatively small lung lesions, and thus requires repeating the puncture to achieve success, which not only reduces the success rate and puncture accuracy, but enhances the possibility of pneumothorax, and also increases operation time and radiation exposure to patients. Once pneumothorax occurs and the lung partly collapses, the difficulty of the puncture will be elevated. In addition, the overlap of the costa and scapula blocks the path of puncture needle, which requires needle adjustments and repeated punctures (Froelich et al., 2002). Furthermore, the clinician has a relatively small region to maneuver in, resulting from limitations of the CT equipment (Jin et al., 2010).

C-arm CT has the advantages of both a DSA perspective and CT, which performs 2-D X-ray projections during C-arm rotation. The projection is recorded by a flat-panel detector and transmitted to the C-arm imaging system to generate a CT-like image. At the same time, the axial, sagittal, and coronal images are reconstructed. A series of post-processing technologies, including maximum intensity projection, volume rendering, shaded surface display, and virtual angioscopy are applied to acquire a 3-D rotating image, a CT-like image, and a 3-D vascular reconstruction image, from which we can observe and analyze the lesion size, shape, structure, and its relation to peripheral tissues from any angle. It facilitates the assessment of the anatomical structure of the lesion and the clinical diagnosis (Gupta et al., 2008; Reiser, 2008; Kamran et al., 2010). Resulting from the great difference in density between lung nodules or tumors and peripheral tissue, the excellent contrast obtained can completely fulfill the requirement for small lung lesion puncture. Higashihara et al. (2011) discovered that there was no significant difference in the detection of lung nodules larger than 8 mm between C-arm CT and traditional CT. C-arm CT can be utilized to guide punctures of lung nodules larger than 8 mm. C-arm CT also allows the clinician to observe the position of the needle-electrode from multiple directions during the surgery, so as to ensure that the ablation range is 0.5-1 cm larger than the tumor margin. Moreover, C-arm CT can precisely distinguish lesions from important surrounding organs and the relationship of the needle-electrode to peripheral structures, which avoids thermal damage to important surrounding structures. It also allows for the timely review of lesions following surgery and observation of the occurrence of complications such as pneumothorax. In addition, C-arm CT can produce 1536 slices with a length of 18 cm in 1 full rotation, and sufficient Z-axis coverage enables the generation of images of the lesion and the peripheral tissue in a single scan (Gupta et al., 2006).

Among the total of 35 RFA surgeries in our research, the puncture success rate of 36 lesions was 100%, which conformed to our expectations. Huang et al. (2010) also confirmed the advantages of C-arm CT in one of their studies, in which they performed percutaneous RFA of 15 lesions in 13 patients under C-arm CT guidance. Before surgery, 3-D reconstructions of lesions by C-arm CT were utilized to determine the surgical plan. DSA rotation was performed to monitor the location of the ablation needle by 3-D reconstruction during the surgery; C-arm CT was applied again to review the lesion and to observe whether complications occurred after the surgery. A total of 14 punctures were successful on the first attempt and the location of the needle-electrode was satisfactory in 15 lesions, which fulfilled the surgical requirement. In RFA, the needle position on the body surface could be preoperatively determined under C-arm

CT guidance, and the needle depth could be measured, which facilitated the procedure. The intraoperative status of the lesion and the ablation needle could be observed in different cross-sections, and the accurate positioning of the needle-electrode after insertion and exposing the electrode could be determined. In addition, intraoperative complications could be detected and treated in a timely manner, with an immediate postoperative evaluation of ablation effect.

It must be emphasized that the density resolution of C-arm CT is inferior to that of CT, and is unable to reach a density resolution of 3 HU as in multi-slice spiral CT (Gupta et al., 2006), or to distinguish the heterogeneity of a tumor (Huang et al., 2010). In addition, C-arm CT can induce striping artifacts in cross-sectional reconstructed images, especially during 3-D rotation scanning with a metal puncture needle. Therefore, image guidance technology should be carefully determined when the clinician desires to identify the internal components of lesions or to distinguish lesion from mediastinum.

At present, it is considered difficult to measure the radiation dose of C-arm CT (Orth et al., 2008), and it is very complicated. Compared to multi-slice spiral CT, C-arm CT lacks a commonly accepted standard for general dose measurements. The comparison of images with the same quality from multi-slice spiral CT and C-arm CT is absent in the current literature, but some researchers have performed preliminary studies: the radiation dose exposure from C-arm CT is lower than that of multi-slice spiral CT in individual scanning of same part. Damet et al. (2010) discovered that a lower dose of radiation was required for C-arm CT than CT during the scanning of target organs, the wrist, and inner ear crystals. Daly et al. (2006) used a craniocere-bral model to measure the radiation dose of C-arm CT and found that in order to acquire ideal images of bone and soft tissue structures, the radiation doses were 3 mGy (0.10 mSv) and 10 mGy (0.35 mSv), respectively, which were lower than that of ordinary craniocerebral CT (2 mSv). To acquire imaging of the chest, the radiation dose from C-arm CT was lower than that of multi-slice spiral CT, which was confirmed by Bai et al. (2012) in their research. In a study by He et al. (2010), the dose for lung scanning was 61.2-130.9 $\mu Gy \cdot mA^{-1} \cdot s^{-1}$ on CT and 33.1-76.7 $\mu Gy \cdot mA^{-1} \cdot s^{-1}$ on C-arm CT. One of the studies by Japanese researchers (Bai et al., 2012) revealed that the effective dose for chest scanning was 0.92 mSv on C-arm CT, while the average effective dose indicated in McCollough (2008) was 5-7 mSv for chest scanning on CT. Braak et al. (2011) demonstrated that the average effective doses were 7.6 and 12.3 mSv for C-arm CT-guided puncture of the upper and lower chest, respectively, which reduced the total dose 13-42% compared to 13.0 and 15.1 mSv for traditional CT-guided puncture of the upper and lower chest. Hirota et al. (2006) also showed that C-arm CT generated less radiation than single-detector spiral CT in abdominal interventional surgeries. Other researchers have studied the radiation dose of C-arm CT-guided lung biopsy. Hwang et al. (2010) discovered that the average effective doses were 4.6 mSv and Jin et al. (2010) showed that the cumulative dose was 271 ± 116 mGy for C-arm CT-guided lung biopsy. In our research, the average cumulative dose and average effective dose for RFA were 187.62 ± 108.46 mGy and 5.50 ± 3.31 mSv, respectively.

Recently, efforts have been made to reduce radiation dose; thus, the clinician should carefully consider the application of C-arm CT and number of scans. C-arm CT imaging volume has been recognized as the most important factor determining the amount of scattered radiation. Because of the lack of a collimator in C-arm CT, it is critical to determine the imaging range to reduce the radiation dose. On the other hand, the reduction of scattered radiation also enables image contrast improvements.

In conclusion, the application of C-arm CT in the RFA of small lung lesions could

provide abundant information and simplify the procedure for the clinician, as well as reduce radiation exposure to both patients and the clinician to some extent, which has been considered a promising feature of image-guided technology. Although C-arm CT has some disadvantages, we believe that it will become a more convenient accessory appliance along with the additional development of technology and the accumulation of experience.

ACKNOWLEDGMENTS

REFERENCES

Bai M, Liu B, Mu H, Liu X, et al. (2012). The comparison of radiation dose between C-arm flat-detector CT (DynaCT) and multi-slice CT (MSCT): a phantom study. *Eur. J. Radiol.* 81: 3577-3580.

Braak SJ, van Strijen MJ, van Es HW, Nievelstein RA, et al. (2011). Effective dose during needle interventions: cone-beam CT guidance compared with conventional CT guidance. *J. Vasc. Interv. Radiol.* 22: 455-461.

Daly MJ, Siewerdsen JH, Moseley DJ, Jaffray DA, et al. (2006). Intraoperative cone-beam CT for guidance of head and neck surgery: Assessment of dose and image quality using a C-arm prototype. *Med. Phys.* 33: 3767-3780.

Damet J, Sans-Merce M, Mieville F, Becker M, et al. (2010). Comparison of organ doses and image quality between CT and flat panel XperCT scans in wrist and inner ear examinations. *Radiat. Prot. Dosimetry* 139: 164-168.

Ferlay J, Shin HR, Bray F, Forman D, et al. (2010). Estimates of worldwide burden of cancer in 2008: GLOBOCAN 2008. *Int. J. Cancer* 127: 2893-2917.

Fernando HC, De Hoyos A, Landreneau RJ, Gilbert S, et al. (2005). Radiofrequency ablation for the treatment of non-small cell lung cancer in marginal surgical candidates. *J. Thorac. Cardiovasc. Surg.* 129: 639-644.

Froelich JJ, Ishaque N, Regn J, Saar B, et al. (2002). Guidance of percutaneous pulmonary biopsies with real-time CT fluoroscopy. *Eur. J. Radiol.* 42: 74-79.

Gupta R, Grasruck M, Suess C, Bartling SH, et al. (2006). Ultra-high resolution flat-panel volume CT: fundamental principles, design architecture, and system characterization. *Eur. Radiol.* 16: 1191-1205.

Gupta R, Cheung AC, Bartling SH, Lisauskas J, et al. (2008). Flat-panel volume CT: fundamental principles, technology, and applications. *Radiographics* 28: 2009-2022.

He W, Huda W, Magill D, Tavrides E, et al. (2010). Patient doses and projection angle in cone beam CT. *Med. Phys.* 37: 2359-2368.

Higashihara H, Osuga K, Azuma T, Nakazawa T, et al. (2011). Detection of pulmonary nodules by C-arm CT using a phantom lung: comparison with CT. *Acta Radiol.* 52: 964-968.

Hirota S, Nakao N, Yamamoto S, Kobayashi K, et al. (2006). Cone-beam CT with flat-panel-detector digital angiography system: early experience in abdominal interventional procedures. *Cardiovasc. Intervent. Radiol.* 29: 1034-1038.

Huang DB, Li XQ, Wen ZX, Zhang J, et al. (2010). The clinical application of three-dimensional reconstruction combined with CT-like image in radiofrequency ablation of thoracic neoplasms. *Contemporary Med.* 11: 159-161.

Hwang HS, Chung MJ, Lee JW, Shin SW, et al. (2010). C-arm cone-beam CT-guided percutaneous transthoracic lung biopsy: usefulness in evaluation of small pulmonary nodules. *AJR Am. J. Roentgenol.* 195: W400-W407.

ICRP (2007). The 2007 recommendations of the International Commission on Radiological Protection. *ICRP publication 103. Ann. ICRP* 37: 1-332.

Jin KN, Park CM, Goo JM, Lee HJ, et al. (2010). Initial experience of percutaneous transthoracic needle biopsy of lung nodules using C-arm cone-beam CT systems. *Eur. Radiol.* 20: 2108-2115.

Kamran M, Nagaraja S and Byrne JV (2010). C-arm flat detector computed tomography: the technique and its applications in interventional neuro-radiology. *Neuroradiology* 52: 319-327.

Manhire A, Charig M, Clelland C, Gleeson F, et al. (2003). Guidelines for radiologically guided lung biopsy. *Thorax* 58: 920-936.

McCollough CH (2008). CT dose: how to measure, how to reduce. *Health Phys.* 95: 508-517.

Orth RC, Wallace MJ and Kuo MD (2008). C-arm cone-beam CT: general principles and technical considerations for use in interventional radiology. *J. Vasc. Interv. Radiol.* 19: 814-820.

Reiser MF (2008). Imaging With Flat-Detector C-Arm Systems. In: Multislice CT (Reiser MF, Becker CR, Nikolaou K

and Glazer G, eds.). Springer Press, Heidelberg, 33-51.

Sharma A, Moore WH, Lanuti M and Shepard JA (2011). How I do it: radiofrequency ablation and cryoablation of lung tumors. *J. Thorac. Imaging* 26: 162-174.

Simon CJ, Dupuy DE, Dipetrillo TA, Safran HP, et al. (2007). Pulmonary radiofrequency ablation: long-term safety and efficacy in 153 patients. *Radiology* 243: 268-275.